UNIVERSIDADE DA CORUÑA

# Ferry para navegación en Lago Ontario

## 15-05

## CUADERNO 3: Diseño de formas

Manuel Fraga Seoane


UNIVERSIDADE DA CORUÑA

**DEPARTAMENTO DE INGENIERÍA NAVAL Y OCEÁNICA**

**PROYECTO NÚMERO 15-05**

**TIPO DE BUQUE: FERRY PARA NAVEGACION EN LAGO ONTARIO CANADÁ.**

**CLASIFICACIÓN, COTA Y REGLAMENTOS DE APLICACIÓN: ABS, USCG, SOLAS, MARPOL, ZONA ECA, ICE CLASS (LOW LEVEL).**

**CARACTERÍSTICAS DE LA CARGA:** 399 PAX EN ASIENTOS, 6 TRAILERS Y 24 TURISMOS SIMULTÁNEAMENTE o 60 TURISMOS SOLO.

**VELOCIDAD Y AUTONOMÍA:** 13 NUDOS, 85% MCR, 10 % MM. SIETE DIAS DE OPERACIÓN. EL PERFIL DE LA NAVEGACION SERA DEFINIDO POR EL ALUMNO EN LA ZONA DE NAVEGACION PREVISTA EN EL LAGO ONTARIO A LA VISTA DE LAS CIUDADES DE CONEXION Y DE LOS BUQUES ALLI EXISTENTES.

**SISTEMAS Y EQUIPOS DE CARGA / DESCARGA: RAMPAS DE PROA Y POPA.**

**PROPULSIÓN: DUAL FUEL.**

**TRIPULACIÓN Y PASAJE: 399 PAX MAS 7 TRIPULANTES.**

Ferrol, marzo de 2016

# Índice

# 1.- Introducción

En el Cuaderno 3, se pretende determinar las formas del buque proyecto, con el objetivo de acercarse a los valores de coeficientes y desplazamientos calculados anteriormente.

Para conseguir esto, será necesario cumplir las siguientes condiciones, en la medida de lo posible:

-Garantizar el espacio adecuado en la cubierta de carga, esto es, dotarla de unas dimensiones suficientes para que los coches y camiones quepan en ella.

-Minimizar la resistencia al avance generada por las formas, es decir, proyectar unas formas que opongan la menor resistencia posible.

-Dotar al buque de la estabilidad necesaria.

Para la consecución de las formas del buque proyecto, se utilizarán dos programas de diseño tales como *AutoCad* y *Maxsurf*. Como se ha conseguido una cartilla de trazado de un buque base, se utilizará como referencia.

Como en los anteriores Cuadernos, se parte de las siguientes dimensiones para el buque proyecto:

| Dimensiones principales | | |
|---|---|---|
| L | 61,00 | m |
| Lpp | 56,54 | m |
| B | 17,8 | m |
| D | 4,73 | m |
| T | 3,07 | m |
| D(cub.sup) | 9,73 | m |
| Cb | 0,400 | |
| Cp | 0,527 | |
| Cm | 0,761 | |
| Desplazamiento | 1236 | t |
| Velocidad | 13 | kn |
| Pasajeros | 399 | |
| Tripulantes | 7 | |

*Tabla 1.- Dimensiones principales.*

# 2.- Diseño de las formas mediante derivación de un buque base

## 2.1.- Justificación

A través de la búsqueda en internet, se ha conseguido un artículo que trata sobre la propulsión de aquellos llamados ferris simétricos dentro de los cuales se encuentra el buque que se está proyectando. En este estudio llamado *Double-Ended Ferries – Propulsive Performance Challenges and Model Testing Verification* (1) se analiza tanto la propulsión como las formas más comunes. El mismo se adjunta como Anexo I.
Estas son los tres planos de formas que analiza el documento como las más comunes para *Double-ended ferries*:

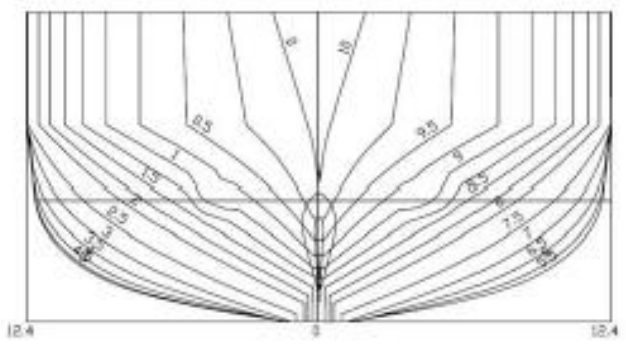

**Figure 1: Round bilge lines**

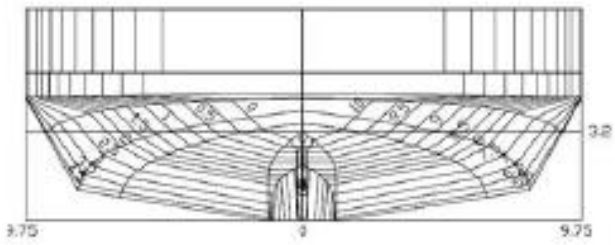

**Figure 2: Double hard chine lines**

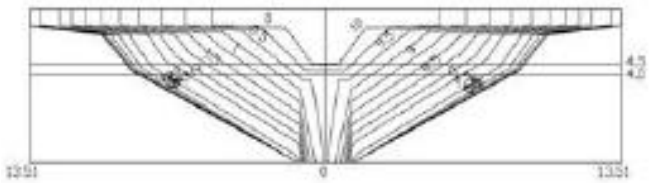

**Figure 3: Single hard chine lines**

*Figura 1.- Formas "Double-ended ferries". Fuente:* (1).

De entre estas tres, se han escogido las “Double hard chine lines”, ya que son lo más parecido a la idea que se tenía para llevar a cabo este proyecto. Para justificarlo, se adjunta, a continuación, un plano longitudinal de un buque perteneciente a la base de datos, el Damen 8521, (no se pudo conseguir otro plano de este buque a pesar de haber contactado con la empresa) para mostrar que se ajusta más a las formas escogidas que a las otras dos:

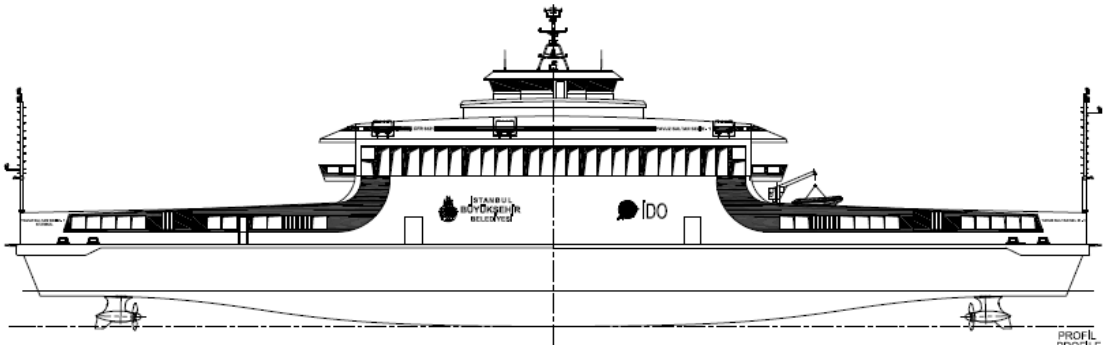


*Figura 2.- Damen 8521. Fuente: Damen 8521* (2).

La principal diferencia entre las formas escogidas como base y este buque de la base de datos es “skeg” o quillote que aparece en las formas base. Este apéndice se incluirá en las formas definitivas, para dotar al buque proyecto de mayor estabilidad transversal.

Cabe destacar que, en las cartillas de trazado que se adjuntarán en apartados siguientes, se incluyen datos del costado que se eleva por encima de la cubierta. Posteriormente, esta parte del casco, no se adjuntará en los planos de formas debido a que no es de gran información a la hora de analizar las propias formas y el comportamiento del casco. También añadir que el valor del puntal máximo del forro en el costado es de 7,6 m en las zonas en las que no hay casetas, en las que hay casetas se alargará hasta la cubierta de pasajeros, a 9,73 m. Las cartillas de trazado se dimensionarán al puntal máximo del forro, ya que las formas de referencia no terminan en la cubierta, si no en el forro de costado.

## 2.2.- Cartilla de trazado adimensional

Se ha utilizado la siguiente imagen para sacar una cartilla de trazado adimensional. Una vez se tuvo impresa, se midieron a mano las mangas y los alturas para cada sección y, posteriormente, se dividió entre la manga máxima y el puntal para que, efectivamente, fuese adimensional.

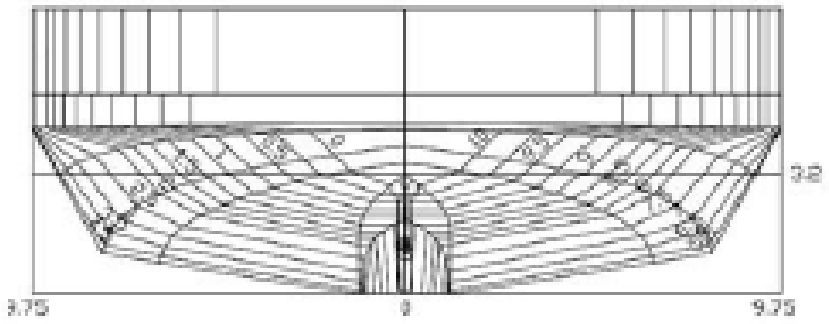


**Figure 2: Double hard chine lines**

*Figura 3.- Plano de formas buque base. Fuente:* (1).

El resultado obtenido fue el siguiente:

| Cartilla de trazado adimensionalizada | | | | | | | | | | | | | | | | | |
|---|---|---|---|---|---|---|---|---|---|---|---|---|---|---|---|---|---|
| Sección 0 | | Sección 0,25 | | Sección 0,5 | | Sección 0,75 | | Sección 1 | | Sección 1,25 | | Sección 1,5 | | Sección 1,75 | | Sección 2 | |
| -36 | | -34,2 | | -32,4 | | -30,6 | | -28,8 | | -27 | | -25,2 | | -23,4 | | -21,6 | |
| Altura | Manga | Altura | Manga | Altura | Manga | Altura | Manga | Altura | Manga | Altura | Manga | Altura | Manga | Altura | Manga | Altura | Manga |
| 0,386 | 0,000 | 0,350 | 0,000 | 0,329 | 0,000 | 0,300 | 0,000 | 0,279 | 0,000 | 0,250 | 0,000 | 0,229 | 0,000 | 0,200 | 0,000 | 0,179 | 0,000 |
| 0,436 | 0,148 | 0,414 | 0,225 | 0,400 | 0,291 | 0,379 | 0,352 | 0,357 | 0,407 | 0,336 | 0,445 | 0,321 | 0,467 | 0,300 | 0,516 | 0,286 | 0,549 |
| 0,486 | 0,187 | 0,471 | 0,275 | 0,457 | 0,346 | 0,443 | 0,412 | 0,429 | 0,473 | 0,414 | 0,533 | 0,393 | 0,577 | 0,371 | 0,626 | 0,357 | 0,659 |
| 0,571 | 0,253 | 0,564 | 0,352 | 0,557 | 0,429 | 0,550 | 0,505 | 0,543 | 0,571 | 0,536 | 0,632 | 0,529 | 0,681 | 0,521 | 0,725 | 0,514 | 0,769 |
| 0,586 | 0,571 | 0,586 | 0,643 | 0,586 | 0,720 | 0,586 | 0,786 | 0,586 | 0,835 | 0,586 | 0,879 | 0,586 | 0,912 | 0,586 | 0,934 | 0,586 | 0,962 |
| 0,700 | 0,571 | 0,700 | 0,643 | 0,700 | 0,720 | 0,700 | 0,786 | 0,700 | 0,835 | 0,700 | 0,879 | 0,700 | 0,912 | 0,700 | 0,934 | 0,700 | 0,962 |
| 0,700 | 0,599 | 0,700 | 0,681 | 0,700 | 0,753 | 0,700 | 0,819 | 0,700 | 0,863 | 0,700 | 0,907 | 0,700 | 0,934 | 0,700 | 0,962 | 0,700 | 1,000 |
| 1,000 | 0,599 | 1,000 | 0,681 | 1,000 | 0,753 | 1,000 | 0,819 | 1,000 | 0,863 | 1,000 | 0,907 | 1,000 | 0,934 | 1,000 | 0,962 | 1,000 | 1,000 |

| Sección 2,5 | | Sección 3 | | Sección 3,5 | | Sección 4 | | Sección 4,5 | | Sección 5 | | Sección 5,5 | | Sección 6 | | Sección 6,5 | | Sección 7 | | Sección 7,5 | |
|---|---|---|---|---|---|---|---|---|---|---|---|---|---|---|---|---|---|---|---|---|---|
| -18 | | -14,4 | | -10,8 | | -7,2 | | -3,6 | | 0 | | 3,6 | | 7,2 | | 10,8 | | 14,4 | | 18 | |
| Altura | Manga | Altura | Manga | Altura | Manga | Altura | Manga | Altura | Manga | Altura | Manga | Altura | Manga | Altura | Manga | Altura | Manga | Altura | Manga | Altura | Manga |
| 0,136 | 0,000 | 0,086 | 0,000 | 0,050 | 0,000 | 0,021 | 0,000 | 0,000 | 0,000 | 0,000 | 0,000 | 0,000 | 0,000 | 0,021 | 0,000 | 0,050 | 0,000 | 0,086 | 0,000 | 0,136 | 0,000 |
| 0,250 | 0,588 | 0,207 | 0,626 | 0,171 | 0,643 | 0,143 | 0,654 | 0,114 | 0,654 | 0,114 | 0,654 | 0,114 | 0,654 | 0,143 | 0,654 | 0,171 | 0,643 | 0,207 | 0,626 | 0,250 | 0,588 |
| 0,321 | 0,714 | 0,271 | 0,758 | 0,229 | 0,786 | 0,186 | 0,802 | 0,150 | 0,813 | 0,150 | 0,813 | 0,150 | 0,813 | 0,186 | 0,802 | 0,229 | 0,786 | 0,271 | 0,758 | 0,321 | 0,714 |
| 0,486 | 0,835 | 0,464 | 0,874 | 0,443 | 0,907 | 0,429 | 0,923 | 0,429 | 0,929 | 0,429 | 0,929 | 0,429 | 0,929 | 0,429 | 0,923 | 0,443 | 0,907 | 0,464 | 0,874 | 0,486 | 0,835 |
| 0,586 | 1,000 | 0,586 | 1,000 | 0,586 | 1,000 | 0,586 | 1,000 | 0,586 | 1,000 | 0,586 | 1,000 | 0,586 | 1,000 | 0,586 | 1,000 | 0,586 | 1,000 | 0,586 | 1,000 | 0,586 | 1,000 |
| 0,700 | 1,000 | 0,700 | 1,000 | 0,700 | 1,000 | 0,700 | 1,000 | 0,700 | 1,000 | 0,700 | 1,000 | 0,700 | 1,000 | 0,700 | 1,000 | 0,700 | 1,000 | 0,700 | 1,000 | 0,700 | 1,000 |
| 0,700 | 1,000 | 0,700 | 1,000 | 0,700 | 1,000 | 0,700 | 1,000 | 0,700 | 1,000 | 0,700 | 1,000 | 0,700 | 1,000 | 0,700 | 1,000 | 0,700 | 1,000 | 0,700 | 1,000 | 0,700 | 1,000 |
| 1,000 | 1,000 | 1,000 | 1,000 | 1,000 | 1,000 | 1,000 | 1,000 | 1,000 | 1,000 | 1,000 | 1,000 | 1,000 | 1,000 | 1,000 | 1,000 | 1,000 | 1,000 | 1,000 | 1,000 | 1,000 | 1,000 |

| Sección 8 | | Sección 8,25 | | Sección 8,5 | | Sección 8,75 | | Sección 9 | | Sección 9,25 | | Sección 9,5 | | Sección 9,75 | | Sección 10 | |
|---|---|---|---|---|---|---|---|---|---|---|---|---|---|---|---|---|---|
| 21,6 | | 23,4 | | 25,2 | | 27 | | 28,8 | | 30,6 | | 32,4 | | 34,2 | | 36 | |
| Altura | Manga | Altura | Manga | Altura | Manga | Altura | Manga | Altura | Manga | Altura | Manga | Altura | Manga | Altura | Manga | Altura | Manga |
| 0,179 | 0,000 | 0,200 | 0,000 | 0,229 | 0,000 | 0,250 | 0,000 | 0,279 | 0,000 | 0,300 | 0,000 | 0,329 | 0,000 | 0,350 | 0,000 | 0,386 | 0,000 |
| 0,286 | 0,549 | 0,300 | 0,516 | 0,321 | 0,467 | 0,336 | 0,445 | 0,357 | 0,407 | 0,379 | 0,352 | 0,400 | 0,291 | 0,414 | 0,225 | 0,436 | 0,148 |
| 0,357 | 0,659 | 0,371 | 0,626 | 0,393 | 0,577 | 0,414 | 0,533 | 0,429 | 0,473 | 0,443 | 0,412 | 0,457 | 0,346 | 0,471 | 0,275 | 0,486 | 0,187 |
| 0,514 | 0,769 | 0,521 | 0,725 | 0,529 | 0,681 | 0,536 | 0,632 | 0,543 | 0,571 | 0,550 | 0,505 | 0,557 | 0,429 | 0,564 | 0,352 | 0,571 | 0,253 |
| 0,586 | 0,962 | 0,586 | 0,934 | 0,586 | 0,912 | 0,586 | 0,879 | 0,586 | 0,835 | 0,586 | 0,786 | 0,586 | 0,720 | 0,586 | 0,643 | 0,586 | 0,571 |
| 0,700 | 0,962 | 0,700 | 0,934 | 0,700 | 0,912 | 0,700 | 0,879 | 0,700 | 0,835 | 0,700 | 0,786 | 0,700 | 0,720 | 0,700 | 0,643 | 0,700 | 0,571 |
| 0,700 | 1,000 | 0,700 | 0,962 | 0,700 | 0,934 | 0,700 | 0,907 | 0,700 | 0,863 | 0,700 | 0,819 | 0,700 | 0,753 | 0,700 | 0,681 | 0,700 | 0,599 |
| 1,000 | 1,000 | 1,000 | 0,962 | 1,000 | 0,934 | 1,000 | 0,907 | 1,000 | 0,863 | 1,000 | 0,819 | 1,000 | 0,753 | 1,000 | 0,681 | 1,000 | 0,599 |

*Tabla 2.- Cartilla de trazado adimensionalizada.*

## 2.3.- Cartilla de trazado aplicando las dimensiones obtenidas del primer dimensionamiento

Esta primera cartilla de trazado se utilizará como referencia en cuanto a coeficientes de arquitectura naval, para tratar de conseguir unos similares cuando se apliquen las dimensiones finales a la cartilla de trazado.

Las dimensiones que se introdujeron en la cartilla de trazado adimensional fueron las obtenidas en el primer dimensionamiento realizado en el Cuaderno 1.

| Dimensiones principales | | |
|---|---|---|
| L | 72 | m |
| B | 15,5 | m |
| D | 4,6 | m |
| D (forro) | 7,6 | m |

*Tabla 3.- Dimensiones principales del primer dimensionamiento.*

A continuación, se adjunta la Cartilla de trazado del buque con las dimensiones anteriores.

| Cartilla de trazado buque proyecto | | | | | | | | | | | | | | | | | |
|---|---|---|---|---|---|---|---|---|---|---|---|---|---|---|---|---|---|
| Sección 0 | | Sección 0,25 | | Sección 0,5 | | Sección 0,75 | | Sección 1 | | Sección 1,25 | | Sección 1,5 | | Sección 1,75 | | Sección 2 | |
| -36 | | -34,2 | | -32,4 | | -30,6 | | -28,8 | | -27 | | -25,2 | | -23,4 | | -21,6 | |
| Altura | Manga | Altura | Manga | Altura | Manga | Altura | Manga | Altura | Manga | Altura | Manga | Altura | Manga | Altura | Manga | Altura | Manga |
| 2,931 | 0,000 | 2,660 | 0,000 | 2,497 | 0,000 | 2,280 | 0,000 | 2,117 | 0,000 | 1,900 | 0,000 | 1,737 | 0,000 | 1,520 | 0,000 | 1,357 | 0,000 |
| 3,311 | 1,150 | 3,149 | 1,746 | 3,040 | 2,257 | 2,877 | 2,725 | 2,714 | 3,151 | 2,551 | 3,449 | 2,443 | 3,620 | 2,280 | 4,003 | 2,171 | 4,258 |
| 3,691 | 1,448 | 3,583 | 2,129 | 3,474 | 2,683 | 3,366 | 3,194 | 3,257 | 3,662 | 3,149 | 4,130 | 2,986 | 4,471 | 2,823 | 4,854 | 2,714 | 5,110 |
| 4,343 | 1,959 | 4,289 | 2,725 | 4,234 | 3,321 | 4,180 | 3,918 | 4,126 | 4,429 | 4,071 | 4,897 | 4,017 | 5,280 | 3,963 | 5,621 | 3,909 | 5,962 |
| 4,451 | 4,429 | 4,451 | 4,982 | 4,451 | 5,578 | 4,451 | 6,089 | 4,451 | 6,473 | 4,451 | 6,813 | 4,451 | 7,069 | 4,451 | 7,239 | 4,451 | 7,452 |
| 5,320 | 4,429 | 5,320 | 4,982 | 5,320 | 5,578 | 5,320 | 6,089 | 5,320 | 6,473 | 5,320 | 6,813 | 5,320 | 7,069 | 5,320 | 7,239 | 5,320 | 7,452 |
| 5,320 | 4,641 | 5,320 | 5,280 | 5,320 | 5,834 | 5,320 | 6,345 | 5,320 | 6,685 | 5,320 | 7,026 | 5,320 | 7,239 | 5,320 | 7,452 | 5,320 | 7,750 |
| 7,600 | 4,641 | 7,600 | 5,280 | 7,600 | 5,834 | 7,600 | 6,345 | 7,600 | 6,685 | 7,600 | 7,026 | 7,600 | 7,239 | 7,600 | 7,452 | 7,600 | 7,750 |

| Sección 2,5 | | Sección 3 | | Sección 3,5 | | Sección 4 | | Sección 4,5 | | Sección 5 | | Sección 5,5 | | Sección 6 | | Sección 6,5 | | Sección 7 | | Sección 7,5 | |
|---|---|---|---|---|---|---|---|---|---|---|---|---|---|---|---|---|---|---|---|---|---|
| -18 | | -14,4 | | -10,8 | | -7,2 | | -3,6 | | 0 | | 3,6 | | 7,2 | | 10,8 | | 14,4 | | 18 | |
| Altura | Manga | Altura | Manga | Altura | Manga | Altura | Manga | Altura | Manga | Altura | Manga | Altura | Manga | Altura | Manga | Altura | Manga | Altura | Manga | Altura | Manga |
| 1,031 | 0,000 | 0,651 | 0,000 | 0,380 | 0,000 | 0,163 | 0,000 | 0,000 | 0,000 | 0,000 | 0,000 | 0,000 | 0,000 | 0,163 | 0,000 | 0,380 | 0,000 | 0,651 | 0,000 | 1,031 | 0,000 |
| 1,900 | 4,556 | 1,574 | 4,854 | 1,303 | 4,982 | 1,086 | 5,067 | 0,869 | 5,067 | 0,869 | 5,067 | 0,869 | 5,067 | 1,086 | 5,067 | 1,303 | 4,982 | 1,574 | 4,854 | 1,900 | 4,556 |
| 2,443 | 5,536 | 2,063 | 5,876 | 1,737 | 6,089 | 1,411 | 6,217 | 1,140 | 6,302 | 1,140 | 6,302 | 1,140 | 6,302 | 1,411 | 6,217 | 1,737 | 6,089 | 2,063 | 5,876 | 2,443 | 5,536 |
| 3,691 | 6,473 | 3,529 | 6,771 | 3,366 | 7,026 | 3,257 | 7,154 | 3,257 | 7,196 | 3,257 | 7,196 | 3,257 | 7,196 | 3,257 | 7,154 | 3,366 | 7,026 | 3,529 | 6,771 | 3,691 | 6,473 |
| 4,451 | 7,750 | 4,451 | 7,750 | 4,451 | 7,750 | 4,451 | 7,750 | 4,451 | 7,750 | 4,451 | 7,750 | 4,451 | 7,750 | 4,451 | 7,750 | 4,451 | 7,750 | 4,451 | 7,750 | 4,451 | 7,750 |
| 5,320 | 7,750 | 5,320 | 7,750 | 5,320 | 7,750 | 5,320 | 7,750 | 5,320 | 7,750 | 5,320 | 7,750 | 5,320 | 7,750 | 5,320 | 7,750 | 5,320 | 7,750 | 5,320 | 7,750 | 5,320 | 7,750 |
| 5,320 | 7,750 | 5,320 | 7,750 | 5,320 | 7,750 | 5,320 | 7,750 | 5,320 | 7,750 | 5,320 | 7,750 | 5,320 | 7,750 | 5,320 | 7,750 | 5,320 | 7,750 | 5,320 | 7,750 | 5,320 | 7,750 |
| 7,600 | 7,750 | 7,600 | 7,750 | 7,600 | 7,750 | 7,600 | 7,750 | 7,600 | 7,750 | 7,600 | 7,750 | 7,600 | 7,750 | 7,600 | 7,750 | 7,600 | 7,750 | 7,600 | 7,750 | 7,600 | 7,750 |

| Sección 8 | | Sección 8,25 | | Sección 8,5 | | Sección 8,75 | | Sección 9 | | Sección 9,25 | | Sección 9,5 | | Sección 9,75 | | Sección 10 | |
|---|---|---|---|---|---|---|---|---|---|---|---|---|---|---|---|---|---|
| 21,6 | | 23,4 | | 25,2 | | 27 | | 28,8 | | 30,6 | | 32,4 | | 34,2 | | 36 | |
| Altura | Manga | Altura | Manga | Altura | Manga | Altura | Manga | Altura | Manga | Altura | Manga | Altura | Manga | Altura | Manga | Altura | Manga |
| 1,357 | 0,000 | 1,520 | 0,000 | 1,737 | 0,000 | 1,900 | 0,000 | 2,117 | 0,000 | 2,280 | 0,000 | 2,497 | 0,000 | 2,660 | 0,000 | 2,931 | 0,000 |
| 2,171 | 4,258 | 2,280 | 4,003 | 2,443 | 3,620 | 2,551 | 3,449 | 2,714 | 3,151 | 2,877 | 2,725 | 3,040 | 2,257 | 3,149 | 1,746 | 3,311 | 1,150 |
| 2,714 | 5,110 | 2,823 | 4,854 | 2,986 | 4,471 | 3,149 | 4,130 | 3,257 | 3,662 | 3,366 | 3,194 | 3,474 | 2,683 | 3,583 | 2,129 | 3,691 | 1,448 |
| 3,909 | 5,962 | 3,963 | 5,621 | 4,017 | 5,280 | 4,071 | 4,897 | 4,126 | 4,429 | 4,180 | 3,918 | 4,234 | 3,321 | 4,289 | 2,725 | 4,343 | 1,959 |
| 4,451 | 7,452 | 4,451 | 7,239 | 4,451 | 7,069 | 4,451 | 6,813 | 4,451 | 6,473 | 4,451 | 6,089 | 4,451 | 5,578 | 4,451 | 4,982 | 4,451 | 4,429 |
| 5,320 | 7,452 | 5,320 | 7,239 | 5,320 | 7,069 | 5,320 | 6,813 | 5,320 | 6,473 | 5,320 | 6,089 | 5,320 | 5,578 | 5,320 | 4,982 | 5,320 | 4,429 |
| 5,320 | 7,750 | 5,320 | 7,452 | 5,320 | 7,239 | 5,320 | 7,026 | 5,320 | 6,685 | 5,320 | 6,345 | 5,320 | 5,834 | 5,320 | 5,280 | 5,320 | 4,641 |
| 7,600 | 7,750 | 7,600 | 7,452 | 7,600 | 7,239 | 7,600 | 7,026 | 7,600 | 6,685 | 7,600 | 6,345 | 7,600 | 5,834 | 7,600 | 5,280 | 7,600 | 4,641 |

*Tabla 4.- Cartilla de trazado del buque proyecto con las dimensiones del primer dimensionamiento.*

Se adjunta como Anexo II el plano de formas del buque con las dimensiones obtenidas en el primer dimensionamiento.

## 2.4.- Cartilla de trazado aplicando las dimensiones finales

Las dimensiones empleadas son las que resultan de la selección final de alternativas.

| Dimensiones principales | | |
|---|---|---|
| L | 61,00 | m |
| B | 17,8 | m |
| D | 4,73 | m |
| D (forro) | 7,6 | m |

*Tabla 5. Dimensiones principales para la selección final.*

| Cartilla de trazado buque proyectado | | | | | | | | | | | | | | | | | |
|---|---|---|---|---|---|---|---|---|---|---|---|---|---|---|---|---|---|
| Sección 0 | | Sección 0,25 | | Sección 0,5 | | Sección 0,75 | | Sección 1 | | Sección 1,25 | | Sección 1,5 | | Sección 1,75 | | Sección 2 | |
| -30,5 | | -28,975 | | -27,45 | | -25,925 | | -24,4 | | -22,875 | | -21,35 | | -19,825 | | -18,3 | |
| Altura | Manga | Altura | Manga | Altura | Manga | Altura | Manga | Altura | Manga | Altura | Manga | Altura | Manga | Altura | Manga | Altura | Manga |
| 2,931 | 0,000 | 2,660 | 0,000 | 2,497 | 0,000 | 2,280 | 0,000 | 2,117 | 0,000 | 1,900 | 0,000 | 1,737 | 0,000 | 1,520 | 0,000 | 1,357 | 0,000 |
| 3,311 | 1,320 | 3,149 | 2,005 | 3,040 | 2,592 | 2,877 | 3,130 | 2,714 | 3,619 | 2,551 | 3,961 | 2,443 | 4,157 | 2,280 | 4,597 | 2,171 | 4,890 |
| 3,691 | 1,663 | 3,583 | 2,445 | 3,474 | 3,081 | 3,366 | 3,668 | 3,257 | 4,205 | 3,149 | 4,743 | 2,986 | 5,135 | 2,823 | 5,575 | 2,714 | 5,868 |
| 4,343 | 2,249 | 4,289 | 3,130 | 4,234 | 3,814 | 4,180 | 4,499 | 4,126 | 5,086 | 4,071 | 5,624 | 4,017 | 6,064 | 3,963 | 6,455 | 3,909 | 6,846 |
| 4,451 | 5,086 | 4,451 | 5,721 | 4,451 | 6,406 | 4,451 | 6,993 | 4,451 | 7,433 | 4,451 | 7,824 | 4,451 | 8,118 | 4,451 | 8,313 | 4,451 | 8,558 |
| 5,320 | 5,086 | 5,320 | 5,721 | 5,320 | 6,406 | 5,320 | 6,993 | 5,320 | 7,433 | 5,320 | 7,824 | 5,320 | 8,118 | 5,320 | 8,313 | 5,320 | 8,558 |
| 5,320 | 5,330 | 5,320 | 6,064 | 5,320 | 6,699 | 5,320 | 7,286 | 5,320 | 7,677 | 5,320 | 8,069 | 5,320 | 8,313 | 5,320 | 8,558 | 5,320 | 8,900 |
| 7,600 | 5,330 | 7,600 | 6,064 | 7,600 | 6,699 | 7,600 | 7,286 | 7,600 | 7,677 | 7,600 | 8,069 | 7,600 | 8,313 | 7,600 | 8,558 | 7,600 | 8,900 |

| Sección 2,5 | | Sección 3 | | Sección 3,5 | | Sección 4 | | Sección 4,5 | | Sección 5 | | Sección 5,5 | | Sección 6 | | Sección 6,5 | | Sección 7 | | Sección 7,5 | |
|---|---|---|---|---|---|---|---|---|---|---|---|---|---|---|---|---|---|---|---|---|---|
| -15,25 | | -12,2 | | -9,15 | | -6,1 | | -3,05 | | 0 | | 3,05 | | 6,1 | | 9,15 | | 12,2 | | 15,25 | |
| Altura | Manga | Altura | Manga | Altura | Manga | Altura | Manga | Altura | Manga | Altura | Manga | Altura | Manga | Altura | Manga | Altura | Manga | Altura | Manga | Altura | Manga |
| 1,031 | 0,000 | 0,651 | 0,000 | 0,380 | 0,000 | 0,163 | 0,000 | 0,000 | 0,000 | 0,000 | 0,000 | 0,000 | 0,000 | 0,163 | 0,000 | 0,380 | 0,000 | 0,651 | 0,000 | 1,031 | 0,000 |
| 1,900 | 5,232 | 1,574 | 5,575 | 1,303 | 5,721 | 1,086 | 5,819 | 0,869 | 5,819 | 0,869 | 5,819 | 0,869 | 5,819 | 1,086 | 5,819 | 1,303 | 5,721 | 1,574 | 5,575 | 1,900 | 5,232 |
| 2,443 | 6,357 | 2,063 | 6,748 | 1,737 | 6,993 | 1,411 | 7,140 | 1,140 | 7,237 | 1,140 | 7,237 | 1,140 | 7,237 | 1,411 | 7,140 | 1,737 | 6,993 | 2,063 | 6,748 | 2,443 | 6,357 |
| 3,691 | 7,433 | 3,529 | 7,775 | 3,366 | 8,069 | 3,257 | 8,215 | 3,257 | 8,264 | 3,257 | 8,264 | 3,257 | 8,264 | 3,257 | 8,215 | 3,366 | 8,069 | 3,529 | 7,775 | 3,691 | 7,433 |
| 4,451 | 8,900 | 4,451 | 8,900 | 4,451 | 8,900 | 4,451 | 8,900 | 4,451 | 8,900 | 4,451 | 8,900 | 4,451 | 8,900 | 4,451 | 8,900 | 4,451 | 8,900 | 4,451 | 8,900 | 4,451 | 8,900 |
| 5,320 | 8,900 | 5,320 | 8,900 | 5,320 | 8,900 | 5,320 | 8,900 | 5,320 | 8,900 | 5,320 | 8,900 | 5,320 | 8,900 | 5,320 | 8,900 | 5,320 | 8,900 | 5,320 | 8,900 | 5,320 | 8,900 |
| 5,320 | 8,900 | 5,320 | 8,900 | 5,320 | 8,900 | 5,320 | 8,900 | 5,320 | 8,900 | 5,320 | 8,900 | 5,320 | 8,900 | 5,320 | 8,900 | 5,320 | 8,900 | 5,320 | 8,900 | 5,320 | 8,900 |
| 7,600 | 8,900 | 7,600 | 8,900 | 7,600 | 8,900 | 7,600 | 8,900 | 7,600 | 8,900 | 7,600 | 8,900 | 7,600 | 8,900 | 7,600 | 8,900 | 7,600 | 8,900 | 7,600 | 8,900 | 7,600 | 8,900 |

| Sección 8 | | Sección 8,25 | | Sección 8,5 | | Sección 8,75 | | Sección 9 | | Sección 9,25 | | Sección 9,5 | | Sección 9,75 | | Sección 10 | |
|---|---|---|---|---|---|---|---|---|---|---|---|---|---|---|---|---|---|
| 18,3 | | 19,825 | | 21,35 | | 22,875 | | 24,4 | | 25,925 | | 27,45 | | 28,975 | | 30,5 | |
| Altura | Manga | Altura | Manga | Altura | Manga | Altura | Manga | Altura | Manga | Altura | Manga | Altura | Manga | Altura | Manga | Altura | Manga |
| 1,357 | 0,000 | 1,520 | 0,000 | 1,737 | 0,000 | 1,900 | 0,000 | 2,117 | 0,000 | 2,280 | 0,000 | 2,497 | 0,000 | 2,660 | 0,000 | 2,931 | 0,000 |
| 2,171 | 4,890 | 2,280 | 4,597 | 2,443 | 4,157 | 2,551 | 3,961 | 2,714 | 3,619 | 2,877 | 3,130 | 3,040 | 2,592 | 3,149 | 2,005 | 3,311 | 1,320 |
| 2,714 | 5,868 | 2,823 | 5,575 | 2,986 | 5,135 | 3,149 | 4,743 | 3,257 | 4,205 | 3,366 | 3,668 | 3,474 | 3,081 | 3,583 | 2,445 | 3,691 | 1,663 |
| 3,909 | 6,846 | 3,963 | 6,455 | 4,017 | 6,064 | 4,071 | 5,624 | 4,126 | 5,086 | 4,180 | 4,499 | 4,234 | 3,814 | 4,289 | 3,130 | 4,343 | 2,249 |
| 4,451 | 8,558 | 4,451 | 8,313 | 4,451 | 8,118 | 4,451 | 7,824 | 4,451 | 7,433 | 4,451 | 6,993 | 4,451 | 6,406 | 4,451 | 5,721 | 4,451 | 5,086 |
| 5,320 | 8,558 | 5,320 | 8,313 | 5,320 | 8,118 | 5,320 | 7,824 | 5,320 | 7,433 | 5,320 | 6,993 | 5,320 | 6,406 | 5,320 | 5,721 | 5,320 | 5,086 |
| 5,320 | 8,900 | 5,320 | 8,558 | 5,320 | 8,313 | 5,320 | 8,069 | 5,320 | 7,677 | 5,320 | 7,286 | 5,320 | 6,699 | 5,320 | 6,064 | 5,320 | 5,330 |
| 7,600 | 8,900 | 7,600 | 8,558 | 7,600 | 8,313 | 7,600 | 8,069 | 7,600 | 7,677 | 7,600 | 7,286 | 7,600 | 6,699 | 7,600 | 6,064 | 7,600 | 5,330 |

*Tabla 6.- Cartilla de trazado del buque proyecto con las dimensiones finales.*

Cabe destacar que en el *Maxsurf* se añadirá el skeg que aparece en el plano de formas obtenido del estudio de propulsión y los cierres (a modo de espejo) de proa y de popa que no existían en las formas anteriores. También es necesario destacar que se retocarán las formas en *Maxsurf*, sección a sección, para eliminar faltas y refinar las mismas.

El cambio más apreciable es la dotación de mayor manga a las zonas de proa y de popa, esto es, el afinamiento se produce más tarde y de forma más brusca, para aprovechar mejor el espacio sobre cubierta.

Se adjuntan como Anexo III los planos de formas finales del buque proyecto.

# 3.- Contornos de proa y popa

Antes de nada, se debe recordar que se está trabajando con un buque simétrico proa-popa, por lo que simplemente es necesario analizar cómo van a ser las formas de proa o de popa, puesto que serán iguales.

Se analizará la parte de proa del buque proyecto. La primera decisión a tomar es la ubicación o no de bulbo.

El bulbo de proa es una protuberancia de la proa; es decir, una extensión de la roda por delante de la perpendicular de proa en su parte más baja.

La decisión sobre la utilización o no del bulbo de proa se hace por consideración de mejoras propulsivas en las distintas situaciones de carga, aunque no se debe olvidar otros aspectos como la posible mejora de comportamiento en la mar, (reducción de pantocazos, potencia requerida con olas, etc.) y el incremento de coste estructural.

Un bulbo apropiado, en lo relativo a la propulsión, actúa de la siguiente forma:

- Reduce la resistencia por formación de olas, al disminuir el tren de olas generado por el buque.

- Reduce la resistencia por olas rompientes, al conseguir menos olas y más amortiguadas.

- Reduce la resistencia residual de carácter viscoso al disminuir los torbellinos de proa.

- Aumenta la resistencia friccional por aumentar la superficie mojada.

El campo de aplicación del bulbo de proa es el siguiente:

$0,65 < Cb < 0,815$

$5,50 < L/B < 7$

$0,24 < Fn < 0,57$

Nuestros datos:

- ✗ Cb = 0,401
- ✗ Lpp/B = 56,54/17,8= 3,18
- ✓ Fn = 13*0,5144/RAIZ(9,81*61) = 0,27

Además, si Cb * B / Lpp > 0,135 no es recomendable poner bulbo.

- 0,4 * 17,8 / 56,54 = 0,126

Por lo tanto, siguiendo estos parámetros no parece recomendable la colocación de un bulbo de proa.

Si se analiza la zona por la que navegará el buque, que es una zona de aguas interiores, el Lago Ontario, se puede aventurar que la resistencia por formación de olas que va a sufrir el buque no va a ser muy importante en cuanto a la resistencia total. Otra causa por la cual no es conveniente la colocación de un bulbo es la no existencia de uno en las formas del buque base, debido a que este tipo de formas, no son propicias para su colocación.

Para las claras del propulsor se utilizan los siguientes valores mínimos:

**Table 3.4.1 Recommended minimum propeller hull clearances**

| Number of of blades | Hull clearances for twin screw, in metres, *see* Fig. 3.4.4 | |
|---|---|---|
| | *e* | *f* |
| 3 | $1{,}20K\,d_P$ | $1{,}20K\,d_P$ |
| 4 | $1{,}00K\,d_P$ | $1{,}20K\,d_P$ |
| 5 | $0{,}85K\,d_P$ | $0{,}85K\,d_P$ |
| 6 | $0{,}75K\,d_P$ | $0{,}75K\,d_P$ |
| Minimum value | 3 and 4 blades, $0{,}20d_P$<br>5 and 6 blades, $0{,}16d_P$ | $0{,}15d$ |

Symbols

$L_R$ and $C_B$ are as defined in Ch 1,5.2

$$K = \left(0{,}1 + \frac{L_R}{3050}\right)\left(\frac{3{,}48C_BP_s}{L_R^2} + 0{,}3\right)$$

$t_R$ = thickness of rudder, in metres measured at $0{,}7R_p$ above the shaft centreline
$P_s$ = designed power on one shaft, in kW
$R_p$ = propeller radius, in metres
$d_P$ = propeller diameter, in metres

NOTE
The above recommended minimum clearances also apply to semi-spade type rudders.

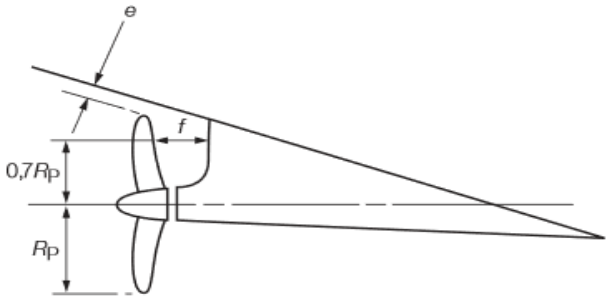


*Figura 4.- Claras mínimas del propulsor. Fuente:* Lloyd's Register (3).

*NOTA: Se utiliza el reglamento Lloyd's Register, debido a que el ABS no dispone nada al respecto.

$$K = (0{,}1 + 59{,}245/3050) * ((3{,}48 * 0{,}4 * 1281{,}88)/59{,}245^2 + 0{,}3) = 0{,}0965$$

El propio reglamento define $L_R$ como:

$$L_R = 0{,}97 * L_{waterline} \text{ ( } en\ buques\ sin\ timón \text{ )}$$

La eslora en la flotación es igual a 59,245, que se adjunta en las hidrostáticas en el apartado siguiente.

En el Cuaderno 6, se estima que la hélice con mejor rendimiento es la de 6 palas, se utilizarán las siguientes fórmulas:

$$e = 0{,}75 * K * dp = 0{,}75 * 0{,}096 * 1{,}8 = 0{,}13\ m$$

$$e = 0{,}16 * dp = 0{,}16 * 1{,}8 = 0{,}29\ m$$

La segunda variante de la ecuación muestra el valor mínimo para la clara que se aplicará si de la primera ecuación resulta un valor menor.

Y en la clara "f":

$$f = 0{,}75 * K * dp = 0{,}75 * 0{,}096 * 1{,}8 = 0{,}13\ m$$

$$f = 0{,}15 * dp = 0{,}15 * 1{,}8 = 0{,}27\ m$$

La segunda variante de la ecuación muestra el valor mínimo para la clara que se aplicará si de la primera ecuación resulta un valor menor.

Se puede comprobar, en el siguiente croquis, que las claras son mayores que las mínimas establecidas. Las cotas son en metros.

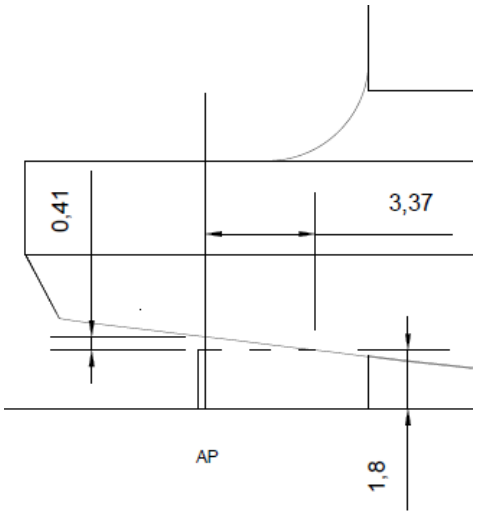


*Figura 5.- Justificación claras mínimas del propulsor*

# 4.- Cálculo de hidrostáticas al calado de diseño y comparación de los coeficientes de forma iniciales y finales

El objetivo de este apartado es tratar de demostrar que los coeficientes de forma finales (con las dimensiones finales una vez retocadas en *Maxsurf)* son del orden de aquellos calculados con las medidas iniciales sacadas del dimensionamiento.

Para ello, se han calculado las hidrostáticas de ambos modelos a su calado de diseño correspondiente. A la izquierda se tienen las de las dimensiones iniciales y a la derecha las de las dimensiones finales.

Hydrostatics at DWL

| | Measurement | Value | Units |
|---|---|---|---|
| 1 | Displacement | 1216 | t |
| 2 | Volume (displaced) | 1216,335 | m^3 |
| 3 | Draft Amidships | 3,080 | m |
| 4 | Immersed depth | 3,080 | m |
| 5 | WL Length | 72,000 | m |
| 6 | Beam max extents on WL | 14,279 | m |
| 7 | Wetted Area | 856,020 | m^2 |
| 8 | Max sect. area | 33,424 | m^2 |
| 9 | Waterpl. Area | 761,003 | m^2 |
| 10 | Prismatic coeff. (Cp) | 0,505 | |
| 11 | Block coeff. (Cb) | 0,384 | |
| 12 | Max Sect. area coeff. (Cm) | 0,760 | |
| 13 | Waterpl. area coeff. (Cwp) | 0,740 | |
| 14 | LCB length | 0,000 | from zero pt. (+ve fw |
| 15 | LCF length | 0,000 | from zero pt. (+ve fw |
| 16 | LCB % | 0,000 | from zero pt. (+ve fw |
| 17 | LCF % | 0,000 | from zero pt. (+ve fw |
| 18 | KB | 2,090 | m |
| 19 | KG fluid | 0,000 | m |
| 20 | BMt | 7,795 | m |
| 21 | BML | 184,918 | m |
| 22 | GMt corrected | 9,885 | m |
| 23 | GML | 187,008 | m |
| 24 | KMt | 9,885 | m |
| 25 | KML | 187,008 | m |
| 26 | Immersion (TPc) | 7,610 | tonne/cm |
| 27 | MTc | 0,000 | tonne.m |
| 28 | RM at 1deg = GMt.Disp.sin( | 209,829 | tonne.m |
| 29 | Length:Beam ratio | 5,043 | |
| 30 | Beam:Draft ratio | 4,636 | |
| 31 | Length:Vol^0.333 ratio | 6,745 | |

Density (water) 1 tonne/m^3

Std. densities 1 tonne/m^3 - Std. Metric fresh water (1000.0 kg/m^3)

Hydrostatics at DWL

| | Measurement | Value | Units |
|---|---|---|---|
| 1 | Displacement | 1190 | t |
| 2 | Volume (displaced) | 1190,413 | m^3 |
| 3 | Draft Amidships | 3,070 | m |
| 4 | Immersed depth | 3,070 | m |
| 5 | WL Length | 59,245 | m |
| 6 | Beam max extents on WL | 16,318 | m |
| 7 | Wetted Area | 877,096 | m^2 |
| 8 | Max sect. area | 38,004 | m^2 |
| 9 | Waterpl. Area | 736,989 | m^2 |
| 10 | Prismatic coeff. (Cp) | 0,529 | |
| 11 | Block coeff. (Cb) | 0,401 | |
| 12 | Max Sect. area coeff. (Cm) | 0,759 | |
| 13 | Waterpl. area coeff. (Cwp) | 0,762 | |
| 14 | LCB length | 0,000 | from z |
| 15 | LCF length | 0,000 | from z |
| 16 | LCB % | 0,000 | from z |
| 17 | LCF % | 0,000 | from z |
| 18 | KB | 2,061 | m |
| 19 | KG fluid | 0,000 | m |
| 20 | BMt | 10,223 | m |
| 21 | BML | 129,373 | m |
| 22 | GMt corrected | 12,284 | m |
| 23 | GML | 131,434 | m |
| 24 | KMt | 12,284 | m |
| 25 | KML | 131,434 | m |
| 26 | Immersion (TPc) | 7,370 | tonne/c |
| 27 | MTc | 28,563 | tonne. |
| 28 | RM at 1deg = GMt.Disp.sin( | 255,198 | tonne. |
| 29 | Length:Beam ratio | 3,631 | |
| 30 | Beam:Draft ratio | 5,315 | |
| 31 | Length:Vol^0.333 ratio | 5,590 | |

Density (water) 1 tonne/m^3

Std. densities 1 tonne/m^3 - Std. Metric fresh water (100

*Figura 6.- Comparación características hidrostáticas*

Por lo tanto, a partir de ahora, las dimensionenes principales del buque serán las que se adjuntan a continuación:

| Dimensiones principales | | |
|---|---|---|
| L | 61,00 | m |
| Lpp | 56,54 | m |
| B | 17,8 | m |
| D | 4,73 | m |
| T | 3,07 | m |
| D(cub.sup) | 9,73 | m |
| Cb | 0,401 | |
| Cp | 0,529 | |
| Cm | 0,759 | |
| Desplazamiento | 1190 | t |
| Velocidad | 13 | kn |
| Pasajeros | 399 | |
| Tripulantes | 7 | |

*Tabla 7.- Dimensiones principales y coeficientes finales.*

Ambos modelos se han ensayado a su calado de diseño, para garantizar un comportamiento de la obra viva lo más parecido posible.

Se puede comprobar la similitud de los coeficientes adimensionales, pero aun así no son exactamente iguales. Esto es debido, en gran parte, a que en los extremos del buque proyecto, se han ancheado las formas, para que pudiese dar cabida a los vehículos en cubierta, es decir, se amplió la zona de cubierta lo que resultó en un aumento de los valores de los coeficientes de bloque, prismático y de flotación. En el caso del coeficiente de maestra el ajuste es muy bueno.

Otro punto en común, es la distribución de la curva de áreas. Los valores no son los mismos en cada punto de la eslora, ya que se ha trabajado con dos eslora distintas, 72 metros y 61 metros. Pero atendiendo a la distribución, se puede predecir un comportamiento similar en ambas carenas.

La primera es la curva de áreas de las formas iniciales.

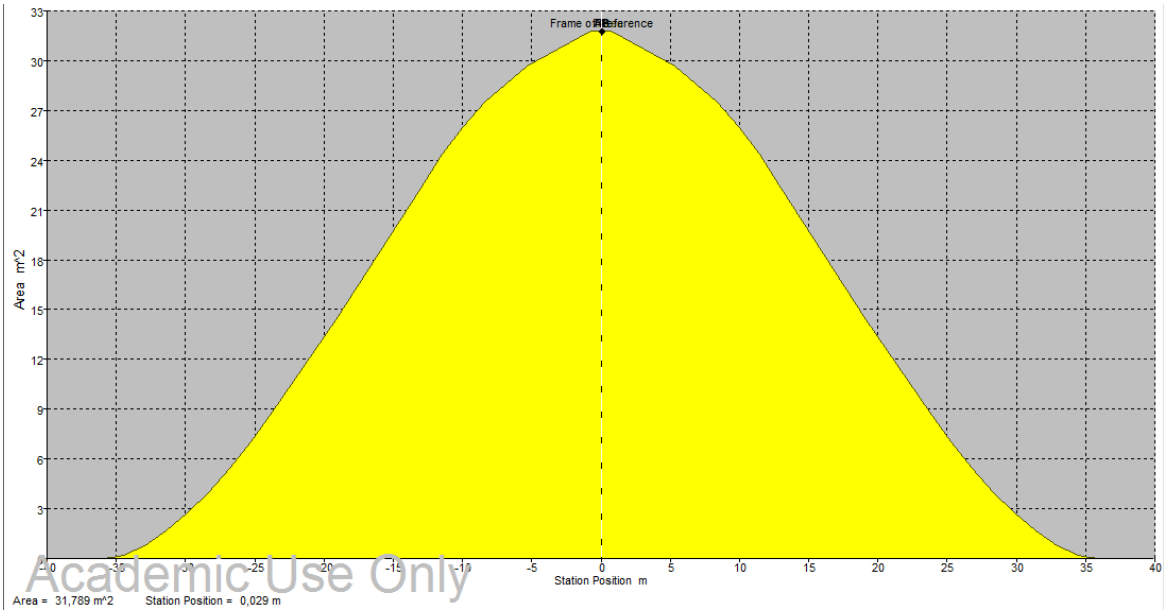


*Figura 7.- Curva de áreas de las formas iniciales*

La segunda es la curva de áreas de las fomras finales. Esta es más redondeada y fina. Se ve un ligero cambio de tendencia a partir de 20 y -20 m, que es debido a la aparición del skeg.

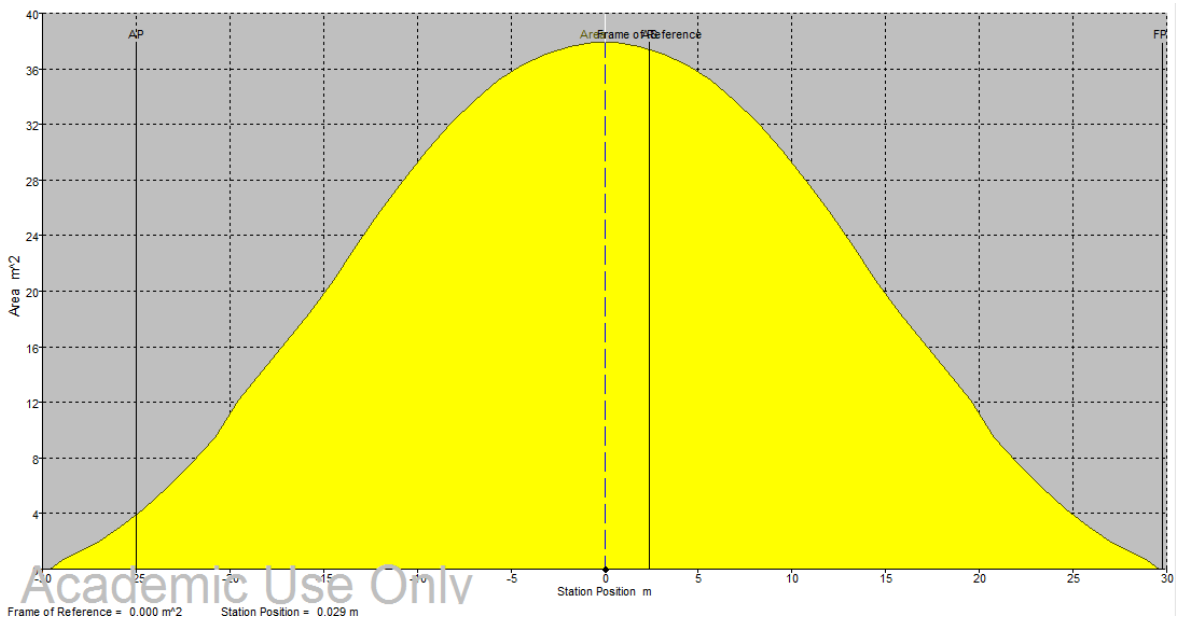


*Figura 8.- Curva de áreas de las formas finales*

# 5.- Bibliografía

1. WA2-2_Minchev.pdf.
2. Damen_Fast_Ropax_Ferry_8521_YN539301_DS.pdf.
3. documents_Rules_NAVAL SHIPS_2015 NAVAL_VOLUME 1_15 Naval_v1 p3.pdf.

# Anexo I. Artículo sobre “Double-ended ferries”

Second International Symposium on Marine Propulsors
smp'11, Hamburg, Germany, June 2011

# Double-Ended Ferries – Propulsive Performance Challenges and Model Testing Verification

**Anton Minchev[1], Claus Simonsen[1], Rune Zilcken[1]**

[1]FORCE Technology (FT), Kgs. Lyngby, Denmark

**ABSTRACT**

For the last two decades Force Technology (FT) has been involved in model testing for a significant number of double-ended ferry designs. The vast collection of geometrical data and still water propulsive performance characteristics for various hull forms (hard chine, round bilge, bulbous bow, etc.) have allowed for some typical trends to be identified and outlined. Furthermore, the increasing importance of pre-testing Computational Fluid Dynamics (CFD) studies in the process of final hull lines definition have proven extremely cost effective and have reduced the number of tested options and conditions.

The objectives of this paper are to present FT accumulated experience in model testing of double-ended ferry hull forms. The following major topics are discussed:

- Contemporary trends in hull lines development and main geometrical particulars.
- Pre-testing hydrodynamic improvement of the hull lines from resistance point of view; application of advanced CFD (wave-making, frictional and form resistance) codes.
- Propulsive performance review and discussion of variable propulsion arrangements; single CL screw, single CL thruster/pod, twin/wing thuster/pod units. Discussion of specific issues like forward-aft (fwd/aft) propeller power optimum distribution; alignment of thruster/pod units with the local flow; propeller submergence and air ventilation.
- Appendage hydrodynamic design; optimization of propeller direction of rotation (for wing propeller systems), streamlining and alignment of pod head-boxes.

The conclusions summarize the major findings of the review, which could serve as a valuable guidelines tool for Naval Architects and Marine Engineers involved in the design, construction and operation of modern double-ended ferries.

**Keywords**

Double-ended ferries, azimuthing thruster/pod unit, multiple-shaft propulsion systems.

## 1 INTRODUCTION

Double-ended ferries constitute a specific class of RO-PAX ships which typically operate on relatively short domestic routes (short crossing periods), confined ferry terminals and in many cases, shallow water conditions. One of the major economic criteria for their efficient operation is the minimum terminal time (harbor maneuvering, berthing and loading/unloading). These requirements call for the specific symmetric hull form and propulsion system, allowing for equally efficient (from a hydrodynamic point of view) sailing ahead and astern, thereby reducing the maneuvering/berthing period. Strictly speaking, the term "sailing ahead/astern" is not applicable here because each end of the ship is either a bow or stern, depending on the direction of sailing.

In view of the above peculiarities, the hydrodynamic optimization of the hull lines and propulsion system faces certain challenges, the successful solution of which needs both CFD studies and model testing verification. Among those, typical design solutions include: optimum hull lines definition for the specific ship speed (Froude number) and water depth, aiming reduction of the hull resistance; appropriate selection of the propulsion system – single CL propellers versus tandem thruster units/pods fwd/aft; adequate design and streamlining of appendages (rudders, fins, thruster head-boxes and streamliners); optimum propeller power distribution between forward/aft propeller groups; optimum alignment of the thruster units (thruster legs) with the local flow.

In the following sections, a brief review of these approaches is presented with illustrations from model test results obtained at Force Technology. Some typical trends and recommendations are outlined.

## 2 SPECIFICS OF LINES AND MAIN PARTICULARAS

During the past decade, Force Technology has model tested a significant number of double-ended ferries. The typical range of main dimensions and design speeds are presented in Table 1.

**Table 1: Range of main dimensions and design speeds for double ended ferries, tested at FT**

| Particular | Unit | Range |
|---|---|---|
| $L_{PP}$ | (m) | 40.0 – 154.0 |
| $L_{WL}$ | (m) | 40.4 – 158.4 |
| $B_{WL}$ | (m) | 9.0 – 26.6 |
| T | (m) | 2.3 – 5.8 |
| Vdesign | (knots) | 12.0 – 21.0 |
| Fn | - | 0.228 – 0.366 |

The typical peculiarities of a double-ended ferry hull lines are: symmetry with respect to mid-ships, hence LCB is centered mid-ships irrespective of the vessel design speed; symmetrical (fwd/aft) propulsion/steering arrangement; frequent operation in relatively shallow water areas implying draught restrictions; required dynamic trim-free operation; symmetrical fwd/aft loading/unloading doors/ramps requiring wider vehicle deck area; priority of good course-keeping ability against maneuverability.

### 2.2 Type of Hull Lines

Typically, two types of hull lines can be distinguished: round bilge and hard chine. These are illustrated in Figures 1, 2 and 3.

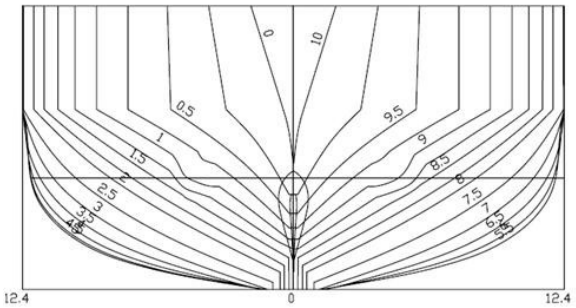


**Figure 1: Round bilge lines**

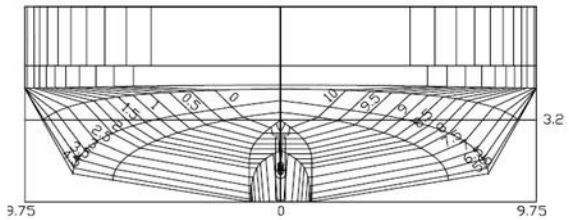


**Figure 2: Double hard chine lines**

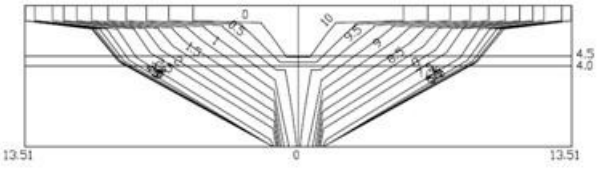


**Figure 3: Single hard chine lines**

Both types are characterized with relatively large $B_{WL}/T$ ratios, pronounced V-shape forward sections, ensuring significant flare to provide sufficient breadth of the loading/unloading ramp and well defined CL skeg to ensure good course-keeping. A challenge for the hard chine lines (either single or multiple chines) is the adequate alignment of the local flow. This will minimize the risk of cross flow and will subsequently ensure separation free flow. A very promising tool for accomplishing this goal is the RANS CFD lines optimization process prior to model testing. This approach is further discussed in Section 3 below.

### 2.3 Propulsion Arrangement

Two typical propulsion arrangements could be distinguished: a single propeller/thruster located at ship's CL fwd/aft, and twin wing thruster/pod units. The first option is naturally combined with a CL rudder fwd/aft, and in some cases, with additional fixed fins for course keeping enhancement. Representative pictures of these two alternatives are illustrated in Figures 4, 5 and 6. The single ducted thruster arrangement in Figure 4 also illustrates the course keeping fin.

**Figure 4: Single ducted thruster unit arrangement**

**Figure 5: Single open propeller arrangement**

**Figure 6: Twin (wing) thruster units arrangement**

The location of the propellers/thrusters/rudders with respect to the ship's hull is mainly dictated by ensuring good inflow into the propeller and rudder, sufficient propeller submergence to minimize the risk of ventilation and last but not least, providing good maneuverability (in case of wing thrusters).

### 2.4 Appendages

Typical appendages for double-ended ferries include skegs, fixed flat fins, bulbous fins, thruster head-boxes and streamliners and sometimes bilge keels and roll damping fins. The skegs are designed and applied mainly to improve course keeping, as in many cases due to low $L_{WL}/B$ and large $B_{WL}/T$ ratios the hull itself could be directionally unstable. Care should be taken not to exceed a reasonable skeg lateral area. In the common case of a classical ship hull (dedicated fwd/aft ends), the larger the skeg area the better course stability. In the case of the symmetrical double ended hull, however, the "bow" skeg will create a side force, which increases the drift angle acting forward of the centre of yaw rotation. In case of insufficient skeg area, the course keeping is enhanced by additional fixed fins, as shown in Figure 4. In this particular case, the fin replaces the rudder, as the steering is accomplished by the azimuthing CL thruster. In some cases, the fin could be constructed more voluminous, resembling a bulb, which contributes to wave-making resistance reduction. An example is shown in the figure below. According to '(Kristensen, 2000)', propulsion power savings of up to 10% were reported based on model test results.

**Figure 7: Illustration of "bulb" fin**

In the case of wing thrusters, the propeller needs to be located as low as possible in order to ensure sufficient submergence, thus avoiding or minimizing the risk of ventilation. This, in many cases, requires an additional thruster head box to house and lower the thruster. The problem of adequate head box streamlining substitutes a significant hydrodynamic challenge and could be attacked both by means of RANS CFD studies, and by physical experiments.

**Figure 8: Illustration of a thruster head box under paint streamline test**

Figure 8 illustrates a typical thruster head box, subjected to paint streamline test to optimize its orientation to the local flow. Care is taken to compromise the orientation between sailing "ahead/astern" conditions, as in these two cases, where there is generally some difference in the local streamlines orientation. Being located close to the free surface, the thruster head box influences not only the frictional and form (pressure) resistance components, but also significantly contributes to the wave-making resistance. A well pronounced head box with additional cone section (to enhance submergence) is illustrated in Figure 9.

**Figure 9: Thruster head box with additional cone**

As seen in the below pictures, this particular head box configuration creates quite substantial fwd/aft local wave system, penalizing the total wave-making of the hull.

**Figure 10: Wave system from FWD thruster head box**

**Figure 11: Wave system from AFT thruster head box**

## 3 RANSE CFD STUDIES

As mentioned above, the double-ended ferries are challenging from a hydrodynamic point of view due to the mid-ship symmetry. For a conventional hull form, the lines in the fore part of the ship must be optimized to have good bow flow properties and the aft lines must be optimized to have good stern flow properties. However, for the double-ended ferry there is no dedicated bow and stern regions since both ends act as bow and stern. Therefore, the hull form optimization must be a compromise of good stern and bow flow properties to make the ship work well.

Making a good double-ended design requires overall knowledge about the resistance of the ship to minimize the fuel consumption as well as detailed insight in the flow field to make sure that the flow around the ship behaves well. Instead of using towing tank testing, which is expensive and time consuming if, for instance, scale models of 3 to 5 design variants have to be built and tested, FT now uses CFD for the pre-testing of the design variants. CFD, which includes form, frictional and wave resistance, can predict the total resistance with an accuracy of 2 to 4 percent compared to model testing, and it provides flow field information beyond what can be measured in the towing tank. Therefore, it is well-suited for the hull form optimization and ranking of design variants in the early design phase. FT uses Star-CCM+ which is a Reynolds Averaged Navier-Stokes Equation (RANSE) solver.

In the following, some examples on applications of CFD for optimization and evaluation of double ended ferries are shown. One of the important things to check in the design phase is the wave making of the ship (see Figures 12 and 13), since this directly influences the wave resistance, and consequently, the fuel consumption.

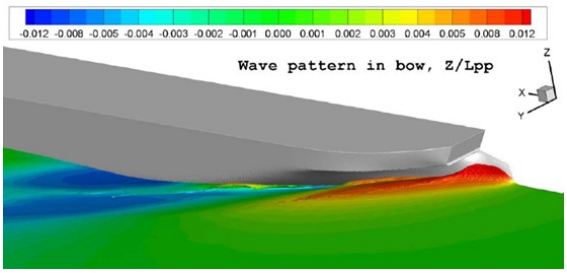


**Figure 12: Computed bow wave**

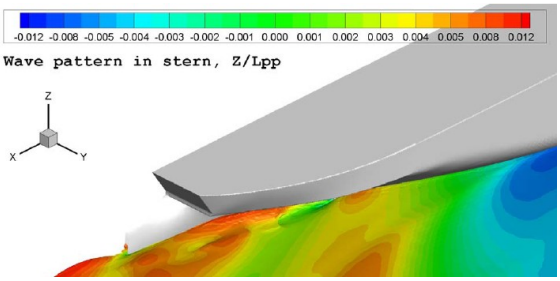


**Figure 13: Computed stern wave**

Aiming at minimizing the wave making of the ship, the naval architect will typically study the computed wave pattern and velocity and pressure fields around the ferry to see how the ship interacts with the water and to get an idea of where the hull or bulbous bow should be modified to change the wave pattern. When the modification has been implemented, the new hull form will be recomputed and the change in wave pattern and resistance will be quantified to judge the influence of the hull form change.

As mentioned earlier, the double-ended ferries can typically be built with round bilge or with hard chine. Both concepts have pros and cons. The hard chine is relatively easy to handle from a production point of view, since it consists of a single curved surface. But, it requires careful work with the hull lines since it must be well aligned with the flow to avoid flow and possibly separation around the sharp corners, which will increase the resistance of the vessel. On the other hand, the round bilge gives a smooth flow in the bilge regions since it is less sensitive to flow alignment. However, it is based on a double curved shape and may be more difficult to produce. To check the alignment of the chine, streamlines are made based on the flow field computed with CFD. If the streamlines follow the chine and make no significant crossing, the design is working, see Figure 14. If it comes to the question whether round bilge or hard chine should be used from a resistance point of view, CFD computations are used to evaluate the resistance difference which can support the decision.

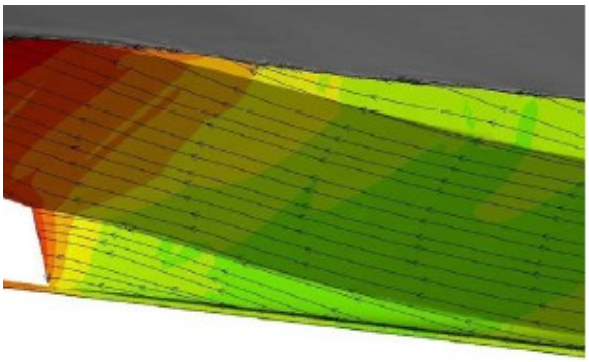

**Figure 14: Check of chine alignment**

A final example of the application of CFD for design and optimization of double ended ferries is related to the propulsion units. If the ferry is equipped with pod units, these are typically mounted on stream lined bodies or thruster head boxes to reduce the drag of the thruster leg and sometimes to prevent air suction, if the propeller is

close to the water surface. A properly working streamliner must be aligned with the flow and should not interact too much with the free surface disturbance in order not to increase the overall resistance of the ship. Aligning the streamliner or head box is tricky on the double-ended ferry since it must work for the ship sailing both ahead and astern and is located in a fairly complex flow field. Conducting the alignment based on model testing is difficult, but CFD offers the possibility to move the head box relatively easy on the model and rerun the configuration to check the alignment and the change in total resistance. Typically, streamlines, flow vectors and hull surface pressure are used for the alignment process. Figures 15 and 16 show examples of the streamline pattern and the hull pressure used for alignment. Further, Figure 16 also shows how the head box interacts with the free surface.

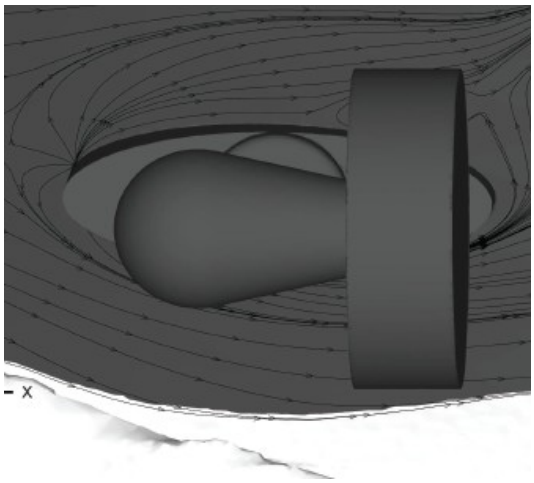


**Figure 15: Streamlines on hull above head box**

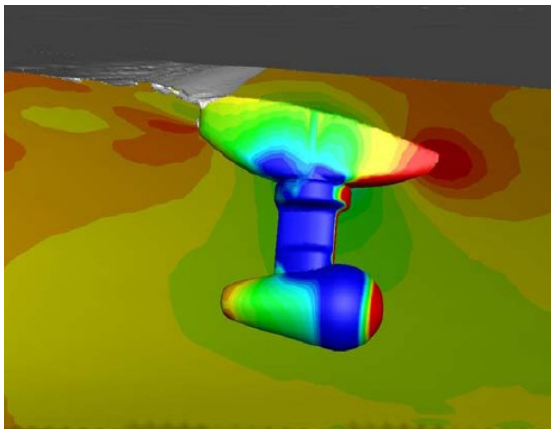

**Figure 16: Pressure on hull surface and head box plus free surface**

When the ferry has been optimized based on the CFD solution, the final design is verified by towing tank testing.

## 4 RESISTANCE DATA

According to established resistance test procedures, the double-ended ferry resistance test is normally performed with appended hull, including rudders, skegs, and eventually, course-keeping fins for the case of single CL propellers, and just the bare hull with thruster head boxes for the case of wing thrusters propulsion. The results are analyzed in accordance with the ITTC-57 correlation line and form factor definition according to the standard Prohaska's method. A summary of derived total ($C_T$) and residual ($C_R$) resistance coefficients are presented in Figure 17. The presented points refer to the design speed condition only for each of the treated designs.

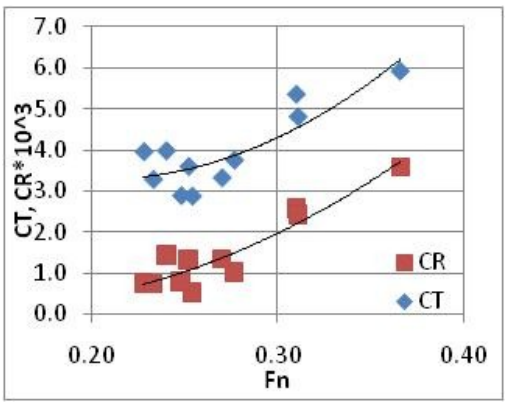


**Figure 17: $C_T$ and $C_R$ versus Froude number**

As seen from Figure 17, the common trend for both $C_T$ and $C_R$ is constant increase with Fn, which is in agreement with common knowledge. The scatter of $C_T$ is a bit larger than the $C_R$ due to the additional effect of the form resistance (form factor) scatter, which is illustrated in Figure 18. From the data in Figure 17, the relative difference between resistance components could be also identified; typically, $C_R$ substitutes from about 30% of $C_T$ at Fn = 0.25 to about 60% of $C_T$ for Fn = 0.35. The rest is attributed to viscous (combined friction and pressure/form) resistance. The illustrated resistance components, together with the trend of form factor behavior, presented in Figure 18, indicate the importance of hull lines optimization process, which aims to reduce both wave-making and viscous resistance components.

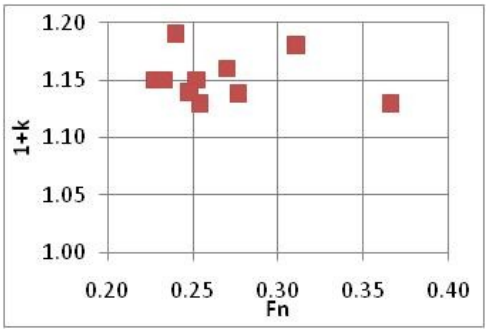


**Figure 18: Form factor versus Froude number**

## 5 PROPULSION DATA

The propulsion tests are performed according to the load variation method, i.e., at each speed the propeller

revolutions (loading) are varied around a predefined towing force $F_D$. The latter compensates for the difference in frictional resistance between model and full scale ship due to the Reynolds number (Rn) difference. During the tests, each propeller thrust (or thruster unit thrust), torque and revolutions are measured together with model speed and applied towing force. Additionally, dynamic sinkage and trim are also recorded. The majority of the propulsion tests are carried out with available stock propellers appropriately selected to closely match with the target pitch and blade area ratios. Prior to the propulsion test, each stock propeller (alone) or as a thruster/pod unit are tested in open water to derive its open water hydrodynamic characteristics. Using those, the effective wake coefficient (w), and the relative rotative efficiency ($\eta_R$) are derived for each propeller (or fwd/aft propeller group) applying thrust identity approach.

The thrust deduction coefficient (t) could be defined either as a global (common) thrust deduction, being average between fwd/aft propellers, or as a separate t for the fwd/aft propeller groups. The latter is strongly recommended. Due to significant differences in the inflow, propeller loading and axial velocity induction, the forward propeller (group) is characterized with significantly higher thrust deduction, governing the propulsive efficiency and influencing the optimum load distribution. The derivation of split fwd/aft thrust deduction can be accomplished, for example, by repeating (after the standard propulsion tests is done) some representative speed points with fwd propellers running at zero thrust, while aft propellers run at their pre-defined loading (RPMs) and vice-versa. Thus, thrust deduction is calculated separately for fwd/aft propeller groups, with the missing thrust (from idling propellers) compensated by the towing force $F_D$ (to be applied nominally as per the defined speed).

### 5.1 Power Distribution

As discussed in Section 2.4 above, two major propulsion arrangements were subject to model testing; single CL fwd/aft propellers and twin wing thruster/pod units. The definition of optimum (in terms of minimum total power consumption at a given speed) power distribution between fwd/aft propeller groups is one of the challenges for double-ended ferry testing. Obviously, the latter is quite project specific and depends on hull lines (local flow conditions), design speed, location of propellers, and appendages and propeller loading.

A typical trend for the power distribution found for single screw ferries is shown in Figure 19. Total power savings of up to 10-12% could be achieved by adequate power distribution. For this class of ferries, the trend indicates minimum power consumption in case of 0%/100% power distribution between fwd/aft propeller. The significant total power increase when the fwd propeller takes part of the load is mainly associated with significant increase of the fwd propeller thrust deduction, associated with increased frictional resistance due to fwd propeller axial flow induction over the ship hull. Such variation of thrust deduction is illustrated in Figure 20. When the fwd propeller is engaged, the aft propeller open water efficiency somewhat increases due to lower propeller loading but not enough to compensate the higher reduction in hull efficiency (through thrust deduction), hence, the significantly higher total power. When the load is distributed 0/100% fwd/aft, the forward propeller will add some resistance penalty, which may account for up to 3-4% of the total resistance. To minimize this additional drag, feathering of the blades (in case of CP propeller) could be recommended, as illustrated in Figure 21, or turning the fwd propeller with small revolutions, corresponding to the zero thrust condition (in case of FP propellers).

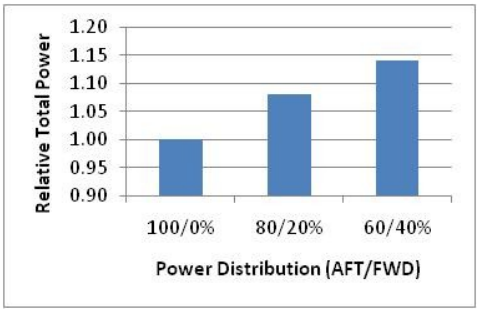


**Figure 19: Example of power saving by power distribution (aft/fwd) – case of single CL propeller**

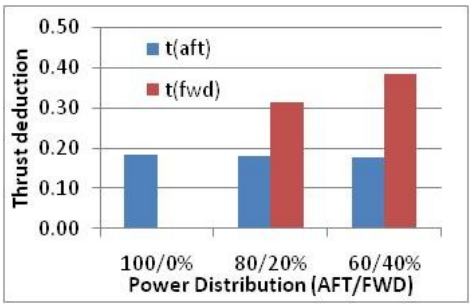


**Figure 20: Example of thrust deduction variation with power distribution – case of single CL propeller**

**Figure 21: Example of feathered FWD propeller**

For the class of twin/wing thruster propulsion systems, typically the forward thrusters take some part of the total power, amounting from 20% to 40% of the total. Again, a

dedicated power distribution test is recommended to obtain the most favorable power distribution (normally this is done for the design speed). An example of power distribution variation is presented in Figure 22, which indicates power saving of about 2.5%, for this particular case. This is relatively lower than the single propeller case and can be probably explained with lower thrust deduction figures for the fwd propeller group. In this case, the propeller jet-flow is not directly hitting the hull, but is diverted a bit aside in the hull boundary layer, hence, a somewhat lower forward thrust deduction. A typical power distribution ratio for wing thruster powered ferries is about 40/60% fwd/aft. Special consideration should be paid to the risk of propeller ventilation (sucking air from free surface). This phenomenon could be, in some cases, effectively controlled by further power distribution variation, aiming minimum loading on fwd/aft propeller groups.

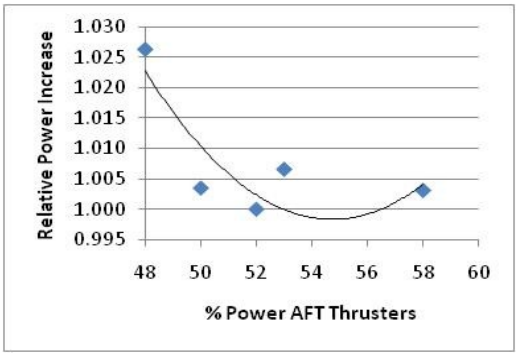


**Figure 22: Example of power saving by power distribution (AFT/FWD) – case of twin wing thrusters**

### 5.2 Thruster Alignment with the Inflow

As discussed in Section 3 above, the flow in way of the fwd/aft trhusters is not symmetrical, hence the need for adequate alignment of the thruster neutral azimuthing or "rudder" angle.

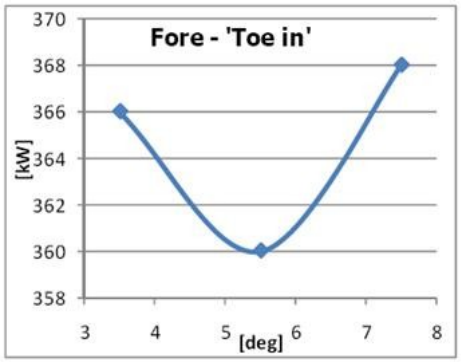


**Figure 23: Variation of FWD propeller power with thruster angle (Fn = 0.229, 2.2% max gain)**

Prior to the model testing phase this could be effectively checked by RANS CFD approach described in Section 3, and finally verified by model test. An example of thruster alignment test is illustrated in Figures 23 and 24. Power savings in the order of 2-3% were achieved in this specific case. The different optimum neutral "rudder" angle fwd/aft, due to the discussed asymmetry of the local flow is to be additionally noted.

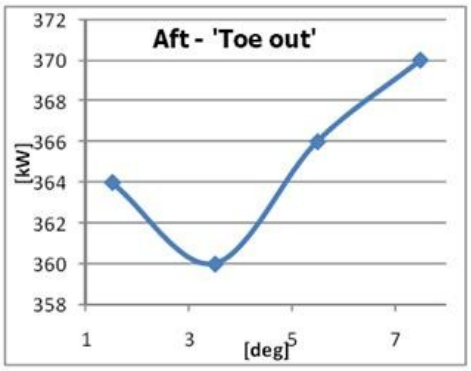


**Figure 24: Variation of AFT propeller power with thruster angle (Fn = 0.229, 2.7% max gain)**

### 5.3 Optimum Propeller Direction of Rotation

Due to the asymmetric propeller wake for wing thrusters, the determination of favorable propeller direction of rotation may be feasible in view of powering optimization. In this case, the propeller rotational induced flow losses could be reduced by utilizing the available pre-swirl (non-zero average tangential in-flow) into the propeller disk. Normally, this is experimentally verified by conducting a short propulsion test (typically at design speed only) where the propeller direction of rotation is consecutively varied, and the better direction is chosen on basis of found minimum total required power. In the case of FP propellers, however, this may not always be practical, because when the ferry direction of sailing is altered, the thruster groups switch their relative placement and turn 180 degrees. Thus, for example, an outward turning aft thruster will become an inward turning forward thruster and vice-versa. Therefore, energy saving potential from propeller direction of rotation selection is relatively modest and based on FT experience could typically amount from 0 to 1.5%.

## 6 CONCLUSION

Double ended-ferries are characterized with symmetric (with respect to mid-ships) lines, characterized with relatively large $B_{WL}/T$ ratios, pronounced V-shape forward sections, ensuring significant flare to provide sufficient breadth of the loading/unloading ramp and well defined CL skeg to ensure good course-keeping. Both round bilge and hard chine sections are typically applied. A challenge for the hard chine sections (either single or multiple chines) is the good alignment with the local flow.

Two typical propulsion arrangements could be distinguished: a single propeller/thruster located at ship's CL fwd/aft, and twin wing thruster/pod units. The first option is naturally combined with a CL rudder fwd/aft.

Typical appendages for double ended-ferries include skegs, fixed flat fins, bulbous fins, thruster head-boxes and streamliners, as well as bilge keels and roll damping fins. The skegs are designed and applied to mainly improve course-keeping, with due consideration of the

altered direction of sailing. The problem of adequate head box streamlining substitutes a significant hydrodynamic challenge and could be attacked both by means of RANS CFD studies, and by physical experiment.

CFD is playing an increasingly important role in the early design phase of double ended ferries, where it is used for lines evaluation prior to tank testing. With its ability to provide quite accurate resistance predictions and very detailed information about the flow field around the ferry, it is a strong tool for optimization and evaluation of the ferry hull lines and appendages. Double-ended ferries are challenging since they have to perform equally good when they sail ahead and astern. Typically CFD is used for overall hull optimization to reduce the wave making, evaluation of round bilge/hard chine solutions and for design and alignment of efficient appendage and thruster head box solutions.

The wave-making resistance component of a double ended ferry hull substitutes from 30% to 60% (depending on Fn) of the total resistance. The viscous (combined friction and pressure/form) resistance component accounts for the rest 70% to 40%. This highlights the importance of the hull lines optimization process, aiming reduction in both wave-making and viscous resistance components.

Thruster head boxes contribute with a major appendage resistance component and require special attention in the design process. Good alignment with the local flow could be achieved both with RANSE CFD and paint streamlines visualization test, preferably accounting for the operating thruster/propeller. Special attention should be also paid to a reasonable compromise in the alignment originating from the altering direction of sailing. Being located close to the free surface, the thruster head box influences not only the frictional and form (pressure) resistance components, but also significantly contributes to the wave-making resistance.

When conducting propulsion tests with double-ended ferries, separate thrust deduction definition for the fwd/aft propeller groups is strongly recommended in order to verify the optimum power distribution and support the final propeller design and optimization.

A typical trend for the optimum power distribution for single CL screw ferries is 0%/100% power distribution between fwd/aft propellers. In the case of wing thrusters propulsion, the more common power distribution is about 40/60% fwd/aft. Special consideration should be paid to the risk of propeller ventilation.

When ferry direction of sailing is altered, the thrusters groups switch their relative placement and turn 180 degrees. Therefore, energy saving potential from propeller direction of rotation selection is relatively modest and based on FT experience could typically amount from 0 to 1.5%.

## REFERENCES

Kristensen, H. O. H. (2000). 'The Maneuverability and Propulsion of Double Ended Ferries. Design Considerations, Construction and Service Experience'. Proceedings of Danish Society of Naval Architects, Copenhagen, Denmark.

# Anexo II. Plano de formas incial (72 m)

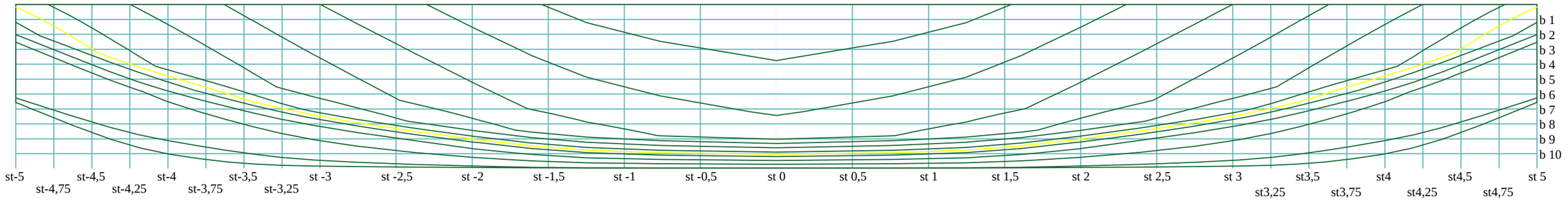


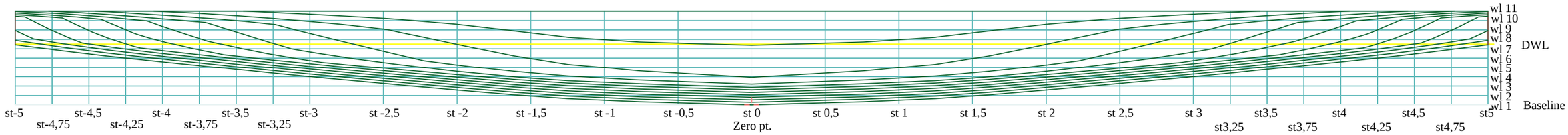


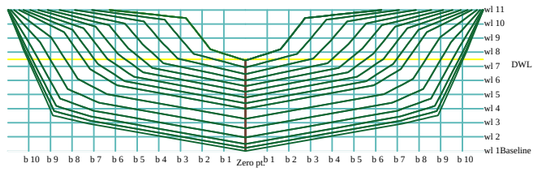


| | |
|---|---|
| Autor: Manuel Fraga Seoane | Plano: Formas 72 m |
| Proyecto: Ferry para navegación en Lago Ontario (Código 15-05) | Escala: 1:200 |

# Anexo III. Plano de formas final (61 m)

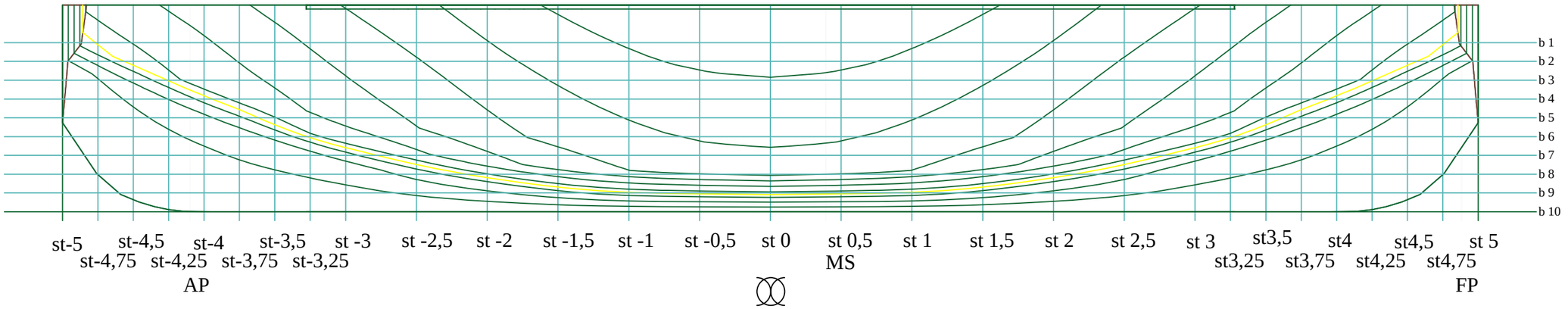


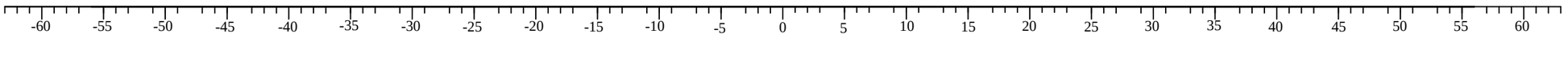


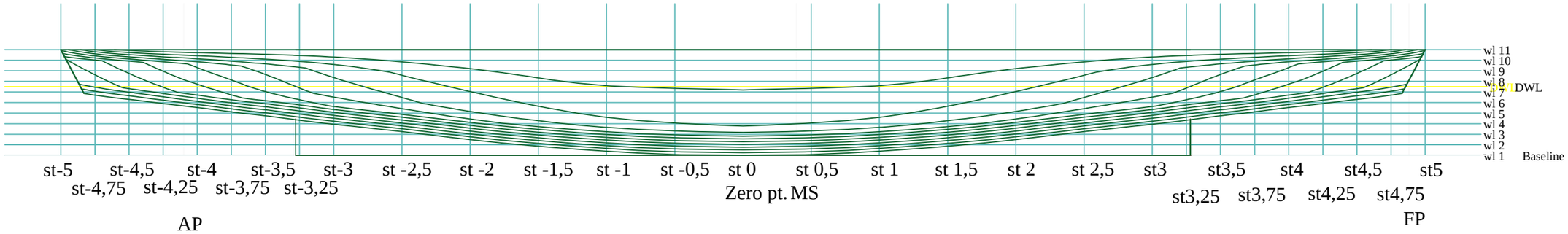


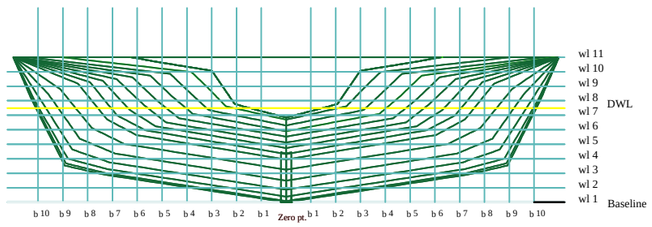


| | |
|---|---|
| Autor: Manuel Fraga Seoane | Plano: Formas finales |
| Proyecto: Ferry para navegación en Lago Ontario (Código 15-05) | Escala: 1:200 |